Application of the V-Notch Shear Test for Unidirectional Hybrid Composites

JIANMEI HE,* MARTIN Y.M. CHIANG,
DONALD L. HUNSTON AND CHARLES C. HAN
Polymers Division
National Institute of Standards and Technology
Gaithersburg, MD 20899, USA

ABSTRACT: The v-notch (Iosipescu) shear test was investigated as a mean for determining the in-plane shear modulus and strength of unidirectional hybrid composites. Two types of hybrid systems having different fiber tow volume fractions composed of carbon and glass fiber tows with epoxy matrix were used for this study. A fiber tow-based finite element analysis was also used to simulate the v-notch shear test for characterizing stress–strain distributions of the specimen. Our experimental and numerical evaluation shows that although the local inhomogeneity inherent in the hybrid composites affects the composite mechanics at a small scale in the v-notch specimen, the test still exhibits a limited region possessing a reasonably pure and uniform stress–strain state between the notches to meet the requirement for a desired shear test. Thus, the study indicates that the v-notch test can be used for the shear testing of the hybrid composites studied when it is correctly used.

KEY WORDS: Iosipescu shear test, v-notch specimen, carbon–glass tow, hybrid composites, shear properties, finite element modeling.

INTRODUCTION

THE INCREASING INTERESTS in hybrid composites (different types of fibers mixed with one matrix material) mostly arise from the ability to combine advantageous features of various fiber systems. For example, users can achieve a significantly better trade-off among various properties between cost and performance. In the development and application of such hybrid composites, complete and accurate understanding of mechanical properties is necessary. Unfortunately, current testing technology is not always adequate to measure or predict the properties of hybrid composites as their properties depend on the microstructure of the hybrids. Especially for shear properties, the situation is much more complex because one of the major problems in shear testing is the influence

*Author to whom correspondence should be addressed.

0021-9983/02/23 2653–14 $10.00/0 DOI: 10.1106/002199802028223

of other stress components besides the shear stress on the final measurements. Therefore, by using experimental evaluation and numerical simulation, this study extends the current application of the v-notch test (also known as the Iosipescu shear test) on non-hybrid composites to hybrid composites for determining the in-plane shear properties (stiffness and strength). This work is limited to a model composite material with unidirectional glass–carbon–epoxy hybrid systems.

The v-notch shear test was originally proposed by Iosipescu [1] for measuring shear strength of isotropic and homogenous materials such as metals. Compared with other test methods, such as the thin-walled tube test and the solid rod torsion test [e.g., 2,3], the v-notch shear test uses a flat specimen that is easier to fabricate while achieving a pure and uniform shear strain–stress state over the test region. Consequently, more reliable results can be obtained, and the test has become well accepted among researchers in the field. In the early 1980s, Walrath and Adams [4] introduced the v-notched shear test to the nonhybrid composite materials. Since then many investigations of the v-notch shear test, as applied to nonhybrid composite materials, have been conducted [e.g., 5–10]. All of these existing experimental and/or theoretical evaluations on the v-notch test are based on nonhybrid fiber–matrix composite systems that were treated as homogeneous media. In our study, the glass and carbon fiber tows are intimately mixed in the epoxy matrix. Such a small-scale combination (exhibits local inhomogeneity), not like nonhybrid composites, can affect the mechanics of the composites and interfere with the test results, particularly in shear. Consequently, the difference in mechanical behavior between the hybrid and nonhybrid composites could be appreciable. Therefore, in this work the v-notch shear specimen with the modified Wyoming test fixture (ASTM D5379-93 [11]) was used to investigate shear properties for unidirectional fiber tow-based hybrid composites (not interply-based hybrid composites).

Two types of hybrid systems (different fiber-tow volume fractions) made of carbon and glass fiber tows were used in this study. For each hybrid system, specimens with tow orientations of 0 and 90° were considered. A fiber tow-based finite element analysis (FEA) of the v-notch specimen is introduced in this work to simulate the mechanical behavior of such hybrid composites. The correction factors needed to compensate for the non-uniformity of shear stress distributions along the cross sections between the two notch tips of the specimens are derived from the finite element analysis for the determination of in-plane shear modulus. Also, failure mechanisms are discussed for v-notch hybrid composite specimens with different fiber tow orientations.

EXPERIMENTS AND NUMERICAL SIMULATIONS OF V-NOTCH SPECIMEN[1]

The modified Wyoming Iosipescu test fixture with the double v-notch specimen and MTS 810 loading cell, shown in Figure 1, were utilized for experimental study. Typical micrographs of sections of a hybrid composite sample are shown in Figure 2, with the bright regions representing the glass–epoxy fiber tows and the dark regions representing the carbon–epoxy fiber tows. The fiber tow is defined as an impregnated tow in this study

[1]Certain commercial materials, equipment and computer code are identified in this paper in order to specify adequately the experimental procedure. In no case does such identification imply recommendation or endorsement by the National Institute of Standards and Technology (NIST) nor does it imply that they are necessarily the best available for the purpose.

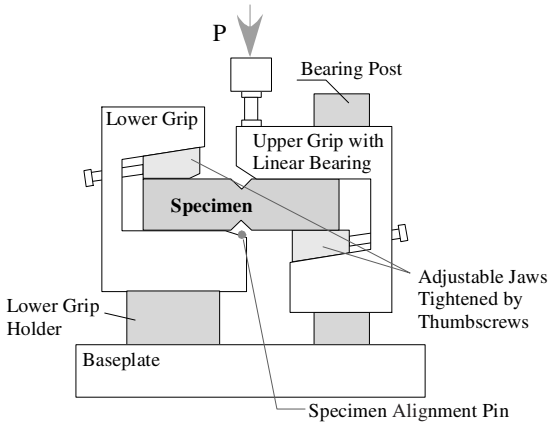

Figure 1. *Schematic of the modified Wyoming shear test fixture with v-notch specimen.*

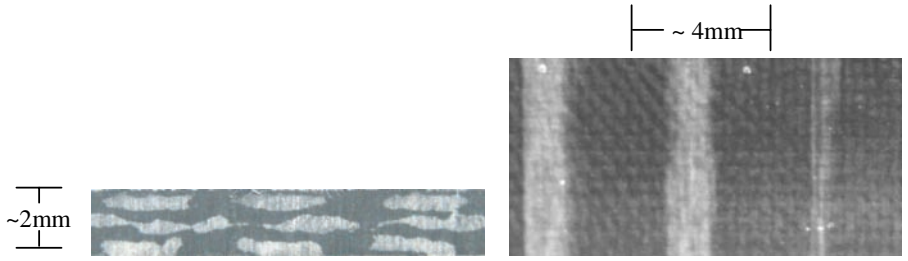

Figure 2. *Photo images of hybrid composite flat samples: (a) cross section; (b) surface.*

Table 1. The fiber tow volume fractions of two hybrid systems used in this study.

Hybrid Composite Systems	Graphite–Epoxy Tow (%)	Glass–Epoxy Tow (%)
Low carbon	33.8	66.2
High carbon	61.8	38.2

(in other words, the fiber tow is taken as a fiber–matrix system rather than a bundle of fibers). Two types of hybrid systems having different volume fractions of fiber–epoxy tows shown in Table 1 (the data are the reported mean values from the manufacturer, Lincoln Composites Inc.; all the numerical simulations are based on these values) were used for the v-notch specimens. As indicated in the table, the ''low carbon'' refers to a hybrid system with lower volume fraction of carbon–epoxy fiber tows (33.8%, defined as the volume fraction of carbon–epoxy tows out of total fiber–epoxy tow volume in hybrid composites), and ''high carbon'' refers to a higher volume fraction of carbon–epoxy fiber tows (61.8%). For both systems, the volume fraction of epoxy matrix of glass–epoxy and carbon–epoxy fiber tows is the same at 30%. Note that this implies that the volume fraction of the epoxy matrix in the hybrid composites is also 30%. The specimen geometry and

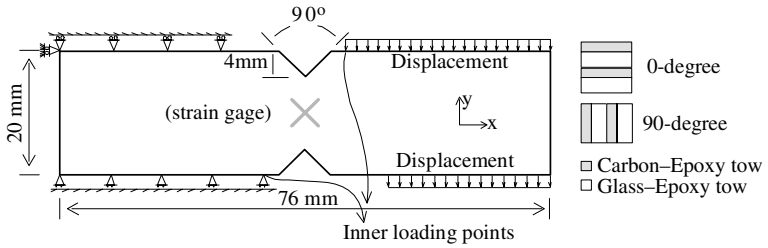

Figure 3. *The v-notch specimen geometry and boundary-loading conditions for finite element analysis. The radius of the notch tips is 1.3 mm.*

loading-boundary conditions for FEA are also displayed in Figure 3. The thickness of specimen is 2.20 mm for high carbon samples, and 2.13 mm for low carbon samples (the standard uncertainty associated with the thickness is 0.01 mm). For each hybrid system, the specimens were cut from the hybrid composite sheets in two different fiber tow orientations: parallel and perpendicular to the longitudinal direction of the specimen as indicated in Figure 3 (referred to as 0 and 90° specimens).

The stacked $\pm 45^\circ$ strain gage rosettes (Micro-measurements CEA-06-120WR-350) are used with the approximate gage size covering an area of $4 \times 4\,\text{mm}^2$ at the test region for the strain measurements. This size, suggested by the result from a separate study on the v-notch test [12], is large enough to cover different types of tows as a representative of the hybrid system.

The average engineering shear strain of the specimen, $\bar{\gamma}$, at the test region can be calculated from the experimentally measured strains at $\pm 45^\circ$ directions (ε_{45° and ε_{-45°) as follows:

$$\bar{\gamma} = \varepsilon_{45^o} - \varepsilon_{-45^o} \tag{1}$$

With the obtained $\bar{\gamma}$ and the average applied shear stress, $\bar{\tau}$ ($\equiv P/A$, where P is the resultant loading force and A is the cross-sectional area between the notch tips), the apparent in-plane shear modulus, $\bar{G}_{12}$, of the hybrid composites can be calculated as:

$$\bar{G}_{12} = \frac{\bar{\tau}}{\bar{\gamma}} \tag{2}$$

$\bar{\tau}$ does not represent the shear stress distribution at the test region covered by the strain gage in the v-notch specimen. Therefore, the correct shear modulus of the hybrid composites, G_{12}, is obtained by modifying $\bar{G}_{12}$ with a correction factor (C) as follows:

$$G_{12} = C\bar{G}_{12} \tag{3}$$

with

$$C = \tau^\circ/\bar{\tau} \quad \text{and} \quad \tau^\circ \equiv \frac{1}{A_o}\int \tau\, dA \tag{4}$$

where $\int \tau\, dA$ represents the integration of the shear stress distribution over the test region, and A_o represents the total area covered by the strain gage. It can be seen that the

correction factor can be only obtained from FEA. Based on results from FEA in [12], the local shear stress at the test region covered by the strain gage is larger than the global average shear stress $\bar{\tau}$ in the 90° specimen, while in the 0° specimen the shear stress is smaller than the global average shear stress $\bar{\tau}$. Therefore, different correction factors for 90 and 0° specimens are needed in the determination of the shear modulus.

The commercial finite element program, ABAQUS [13], was used to simulate the v-notch shear test. The hybrid composites specimens were modeled as two-phase material systems in the FEA (fiber tow-based modeling) based on the configurations shown in Figure 2, with the exact geometry and loading-boundary condition as shown in Figure 3. The whole v-notch specimen was modeled in FEA because of the asymmetric boundary-loading conditions. For the best accuracy, the specimen should be modeled using a three-dimensional (3-D) FEA. Approximately 10,000, eight-node solid elements were used in the modeling of v-notch specimens with two fiber tow orientations: 0 and 90°. The FEA mesh with dimensions continuously decreased towards the notch tips are displayed in Figure 4. It was concluded from this study that good convergence of local stress is achieved.

Experimentally, it is very difficult to obtain all the material properties for each type of fiber tow. Therefore, the input requirements of each tow-based material properties for the FEA were calculated from the rule-of-mixtures based on each constituent properties listed in Table 2. The calculated tow properties are also listed in the table. The longitudinal modulus, E_{11}, was predicted from a general rule-of-mixtures [14]. A modified

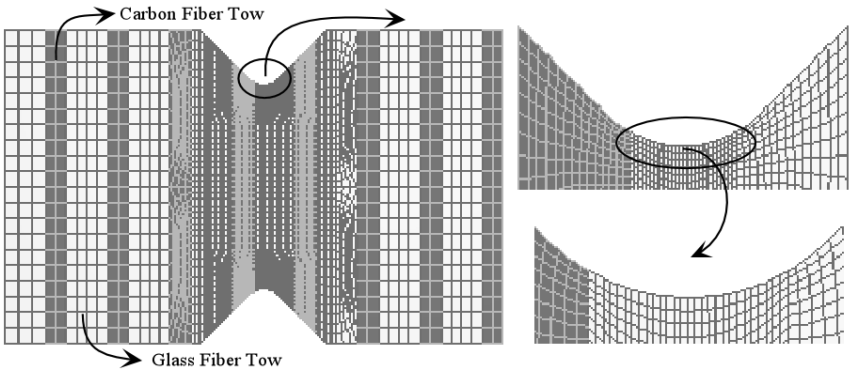

Figure 4. *The finite element mesh of v-notch specimen for fiber tow-based hybrid composites.*

Table 2. The elastic properties of fibers and fiber-tows.

Elastic Modulus	Glass Fiber (GPa)	Graphite Fiber (GPa)	Epoxy Resin (GPa)	Glass Fiber Tow[a] (GPa)	Graphite Fiber Tow[a] (GPa)
E_{11}	72.70	234.90	3.00	51.79[a]	165.33[a]
E_{22}	72.70	13.80	3.00	10.05[b]	7.49[b]
ν_{12}	0.22	0.20	0.40	0.27[a]	0.26[a]
G_{12}	29.98	28.80	1.07	5.08[b]	5.03[b]

[a]the rule-of-mixtures predictions with 30% of the matrix volume fraction in fiber tow; [b]the modified rule-of-mixtures predictions with 30% of the matrix volume fraction in fiber tow.

rule-of-mixtures prediction for the transverse modulus, E_{22}, and shear modulus, G_{12}, were used because of the Poisson's ratio effect between the monolithic fiber and matrix.

Prior to the FEA of v-notch specimens, three-point bend tests [15] for measuring the longitudinal and transverse moduli (E_{11} and E_{22}) for the two hybrid systems were performed to verify the fiber tow-based hybrid modeling. The beam specimens for the three-point bending test were cut from the same hybrid composite sheets. Figure 5 presents two schematic finite element models of the three-point bending test with different fiber tow orientations for E_{11} and E_{22} measurements. Experimental and FEA results for both high and low carbon samples are listed in Table 3. The data in the table indicates that the general trend in the measurements and tow-based FEA predictions on the modulus for different hybrid systems are rational. For the transverse direction, the modulus decreases while the carbon content increases. This is simply because glass fibers generally have higher transverse modulus (treated as isotropic material) compared to carbon fibers. Consequently, they have greater contribution to the transverse modulus than the carbon fiber. One can also see that in general there are reasonably good agreements between experimental measurement and finite element prediction, although there is a little discrepancy in E_{11} (about 15%). This can be explained from the fiber tow offset effect on the elastic moduli shown in Figure 6 obtained by using Tsai's offset modulus results [14]. From this figure one can see that just about 5° of the fiber tow offset causes as much as 15% discrepancy in the measurement of E_{11}. Therefore, these agreements have verified the fiber tow-based finite element modeling on hybrid systems. The experimental results of E_{11} and E_{22} were calculated from the analytical beam solution using the applied load and measured deflection from the three-point bending test.

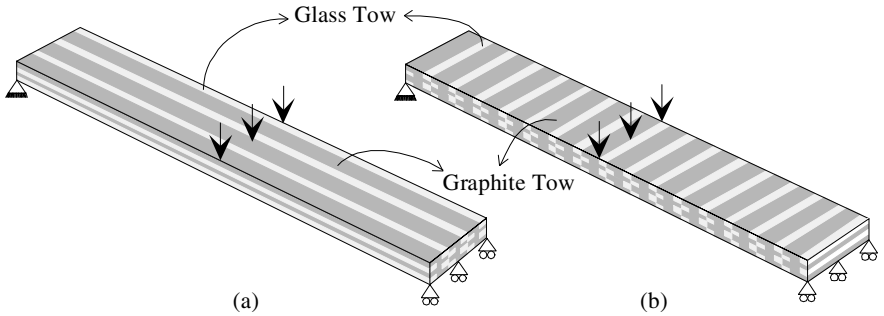

Figure 5. *The three-point bending model for elastic modulus E_{11} and E_{22} measurements of hybrid composites: (a) model for E_{11}; (b) model for E_{22}.*

Table 3. Shear moduli of hybrid composites*.

	Low Carbon Sample (GPa)		High Carbon Sample (GPa)	
Elastic Modulus	**3-D FEA**	**Three-Point Bending Test**	**3-D FEA**	**Three-Point Bending Test**
E_{11}	90.2	83.3 ± 0.77	122.0	101.6 ± 2.0
E_{22}	9.1	9.5 ± 0.05	8.4	8.4 ± 0.27

*The values after the (±) in all the tables refer the standard uncertainty of the measurement.

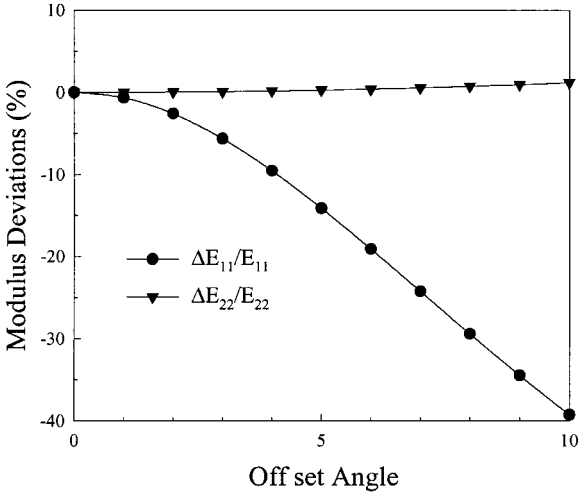

Figure 6. *The deviations of elastic modulus caused by the fiber tow orientations.*

RESULTS AND DISCUSSIONS

General Information on Shear Strain–Stress State

Typical shear stress–strain curves obtained from the v-notch shear tests for both 0 and 90° specimens are shown in Figure 7. Although the figure is obtained for a high carbon hybrid system, the stress–strain curve for a low carbon hybrid system is nearly identical. For 0° specimens, the shear stress–strain relationship is moderately linear up to about 1% of shear strain, where the first load drop was observed. By increasing the loading, sequential load drops were observed until specimen rupture, which is caused by severe crush at the inner loading points. For the 90° specimens, there is also a nearly linear relationship between shear stress and strain up to the approximately 1% of shear strain, where the specimens completely ruptured and no further stress–strain information could be recorded. Moreover, it was observed that the slope of the stress–strain curve in this case is less steep than the 0° specimen. Detailed discussions on measurements of shear modulus and strength are reported in the following sections. Furthermore, we used the tabbed specimens as suggested in the ASTM D 5379, and still experienced similar observations since the tabs eventually would come off (debonding) before the specimen reached a desired failure.

Shear Modulus Determination

For all specimens, the apparent shear moduli, $\bar{G}_{12}$, were conclusively calculated based on the slope of the shear stress–strain curve at the strain ranging from 0.1% to 0.3%, and the results are listed in Table 4. Also listed in this table are the corrected shear moduli G_{12} and FEA predictions. The shear modulus G_{12} is obtained from Equation (4) with $\bar{G}_{12}$ and correction factors calculated from FEA. The correction factor is 0.90 for 0° specimen and 1.09 for the 90° specimen. Within experimental uncertainties, there is generally an acceptably good agreement between the experimental measurements and

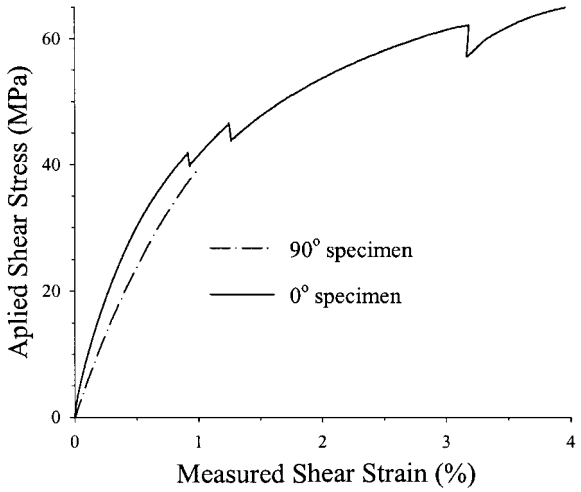

Figure 7. *Typical shear stress–strain curves obtained for 0 and 90° v-notch specimens.*

Table 4. In-plane shear moduli of hybrid composites.

Hybrid Composite Systems		$\bar{G}_{12}$ (GPa)	G_{12} (GPa)	FEA Prediction (GPa)
Low carbon samples	0° specimen	6.78 ± 0.32	6.03 ± 0.28	5.07
	90° specimen	4.87 ± 0.17	5.34 ± 0.19	5.07
High carbon samples	0° specimen	6.48 ± 0.41	5.90 ± 0.37	5.05
	90° specimen	5.09 ± 0.18	5.48 ± 0.19	5.05

FEA predictions for all of hybrid composite systems studied here. As expected, the experimental results and the predictions are independent of the tow orientations used. It is also noted from the table that the FEA predictions for the shear modulus are independent of carbon contents. This demonstrates that the shear modulus of the composites is dominated by the epoxy resin, which is the same at 30% for both low and high carbon hybrid systems.

Interestingly, the experimental results for modulus of 90° specimens are better than the results for the modulus of 0° specimens. This discrepancy can be attributed to the influence of other strain components besides the shear on the strain measurements. Figure 8 gives the principle stress directions calculated from FEA for the elements along the 45° direction, where the strain gage is aligned, in the test region for both 0 and 90° specimens. The deviation of the principal direction from 45° indicates the existence of stress other than intended shear. From this figure, one can see that for 90° specimens there is almost no deviation of the principal direction in the strain gage (covering an area of $4 \times 4\,\text{mm}^2$ at the test region) used here. However, for 0° specimens, the deviation is much higher. Also, the effect of the deviation on the modulus measurement can be demonstrated using long and short strain gages for 90° specimens. Figure 9 presents stress–strain curves of a typical 90° specimen at the strain range from 0.1 to 0.2% for different gage lengths. It can be noted, from the slope of the curves, that using gage size covering an area larger than that of $4 \times 4\,\text{mm}^2$ gives higher value of the apparent shear modulus. The results in Figures 8 and 9

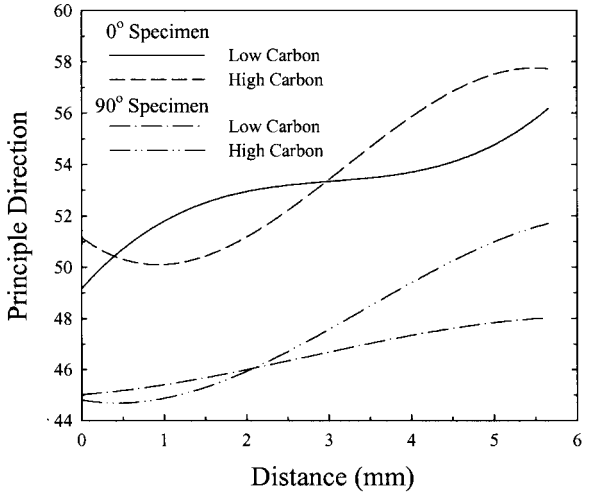

Figure 8. *The principal directions along the strain gage direction (45°) from the specimen center calculated from FEA.*

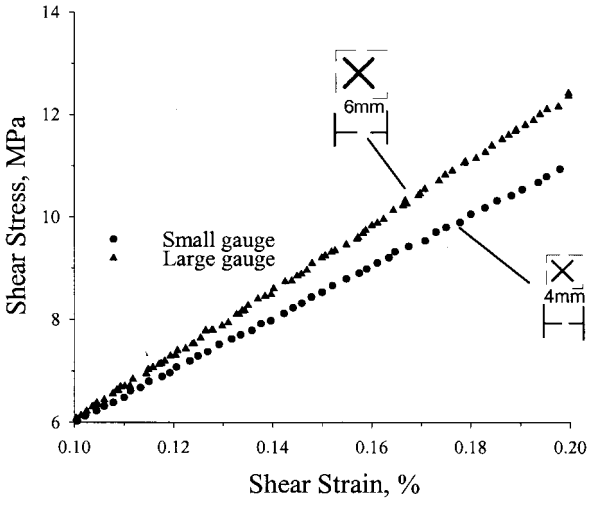

Figure 9. *Typical stress–strain curves at the strain ranging from 0.1 to 0.2% for different gage lengths (90° specimen).*

imply that the v-notch specimens exhibit a limited region where the influence of local inhomogeneity inherent in the hybrid composites on the measurements can be neglected.

A nonlinearity is observed in the shear stress–strain curves for both the 0° and the 90° specimens presented in Figure 7, especially in the 0° specimens. One may argue that this apparent nonlinearity is due to plastic deformation in the resin. However, we speculate that this is due to the micro cracks or micro damages, or local fiber instability before the major rupture events that will be discussed later. The apparent nonlinear behavior starts from the lower level of the shear strain (around 0.5%) of the hybrid composite. The corresponding shear strain level in the epoxy matrix is estimated to be less than 2.5%,

since the shear modulus of the hybrid composites (≈ 5.0 GPa) is about five times higher than the epoxy resin (≈ 1.0 GPa, Table 2). However, the shear yield strain for epoxies is generally around 6% [16]. Therefore, we believe that the epoxy resin does not exhibit plasticity at the shear strain range of the measurements.

Shear Strength Measurements

As mentioned previously in Figure 7, we observed a catastrophic failure in 90° specimens once the shear strain reached about 1%. Crack initiation was observed at the point opposite to the inner loading points (see Figure 3), near the intersections of the upper notch root and straight flank, not at the notch tips, and the crack aligned to the tow direction as shown in Figure 10(a). Once the crack initiated, it would propagate through the specimen and cause complete failure (see Figure 10b). Based on our analytical study [12], the 90° specimen exhibits purer and more uniform shear strain distribution over the test region covered by the strain gages. Therefore, one may expect the 90° specimen to produce better shear strength data. However, the early failure around the notch root area in the 90° specimen makes it impossible to measure the shear strength.

For the 0° specimens, when the shear strain reaches about 1%, crack initiation occurs. The crack was also located opposite to the inner loading points near to the intersection of the upper notch root and straight flank, and the crack was parallel to the tow direction as shown in Figure 11. Once the crack initiated, it would propagate. However, the propagation of the crack would be arrested. When the load was increased, a second crack initiation was observed in a very similar location as the first crack but in another notch root. The locations of the first and second cracks are basically asymmetric. Similar to the behavior observed in the first crack, the second crack was also arrested after some propagation. These two crack initiations correspond to the first and second load drops in the stress–strain curve shown in Figure 7. Under further loading, these two cracks propagated along the fiber tow direction and stopped in the zone underneath the loading fixture. We attribute this arrest to a high compressive stress caused by the loading fixture as well as a low shear stress when cracks propagated into the zone. By continuously

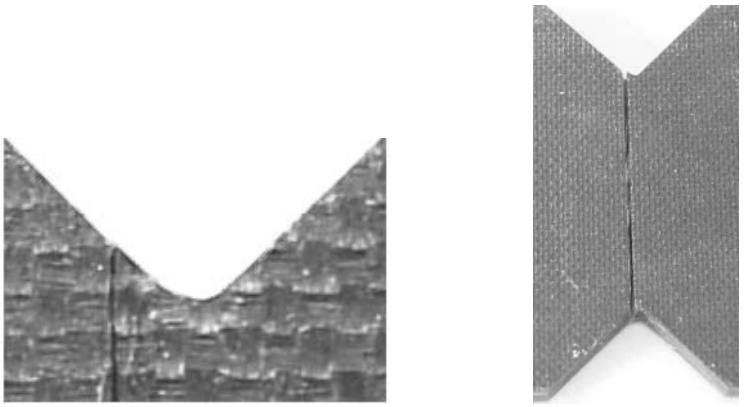

(a) (b)

Figure 10. *Images of crack and rupture for the 90° specimen: (a) initial location; (b) rupture.*

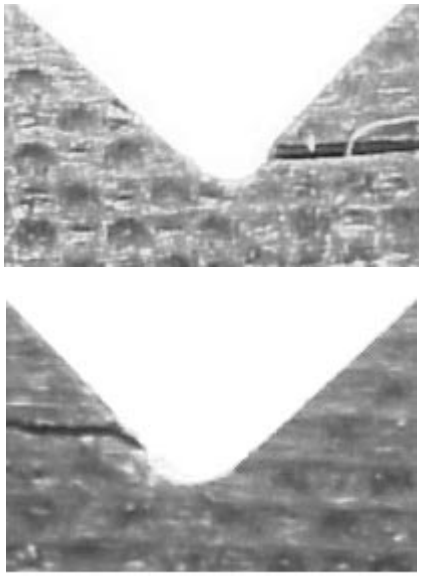

Figure 11. *Photo images showing first and second cracks at notch roots for the 0° specimen.*

increasing the loading, crush of material occurred at the inner loading points due to the stress concentration. So the latter loading drops could possibly correspond to the material crush at inner loading points or more cracks occurred around the notch roots instead of the center region between the notches. Therefore, although there is a theoretical modification in the shear strength determination to compensate for the poor purity and uniformity of the shear stress state in 0° [12], one still cannot get a desired failure in test region.

To better understand the stress state at these locations where the cracks initiated, FEA results for stress distributions around the notch roots are shown. Figure 12 shows the normalized stress distributions around the notch root of 90 and 0° specimens, respectively. It can be seen that the maximum value of these stress components occurred near the intersections of the notch root and straight flank, where it almost coincides with the crack locations observed in experiments shown in Figures 10 and 11. This implies that the failure initiations in both 90 and 0° specimens were due to the stress concentration near the notch roots.

Figure 12(a) shows the stress distribution for the 90° specimen, where σ_x represents the stress in transverse direction to the fiber tow, σ_y the stress in longitudinal direction of the tow, and τ_{xy} the in-plane shear stress. The σ_x is larger than the other two stress components. The crack is observed to be perpendicular to σ_x (Figure 10). The strength of composite in fiber tow orientation is much higher than that in transverse direction, and fibers do not contribute significantly to the shear strength in transverse direction. Therefore, we conclude that the initial failure is in the epoxy resin phase, either inside the tow or between tows, caused by σ_x or τ_{xy}. Due to the lower transverse strength of unidirectional composites in tension and higher normal stress σ_x (about 1.33 times that of the shear component), one can speculate that the crack initiation near the notch root for the 90° specimens is dominated by the crack opening mode, instead of the intended shear mode.

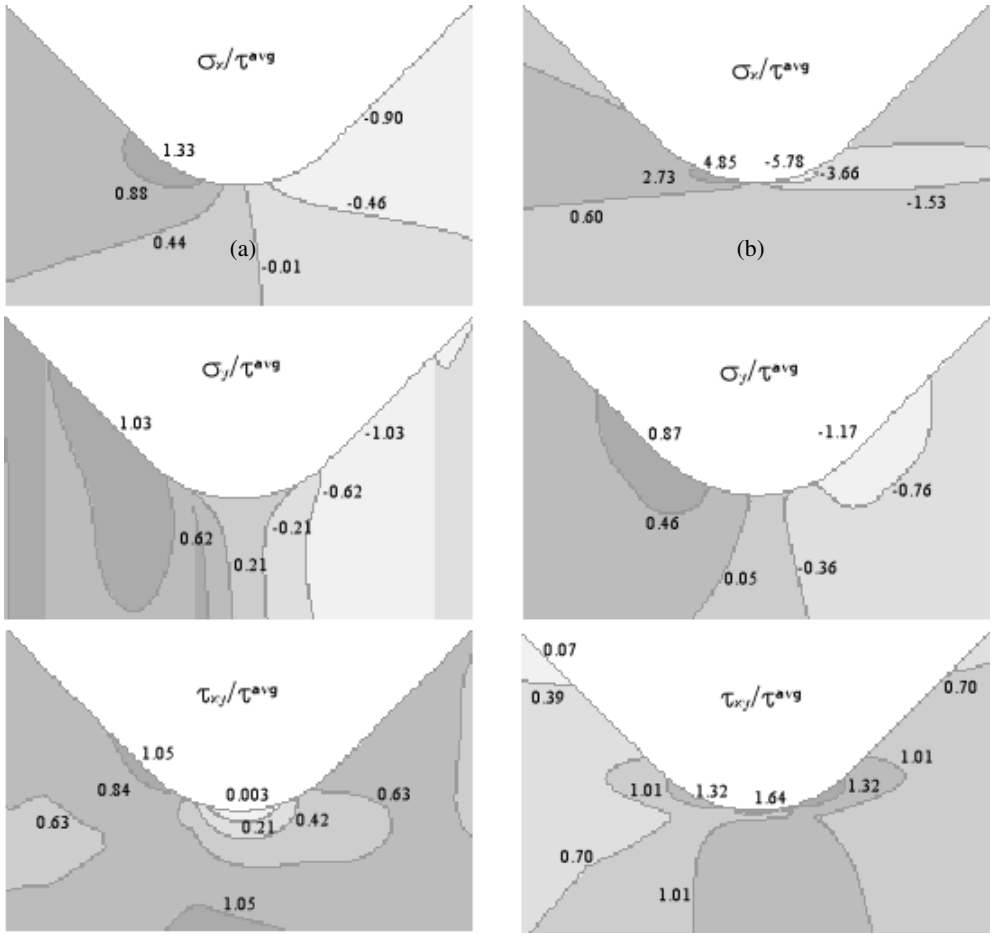

Figure 12. *The contours of normalized stress distributions around the notch roots: (a) 90° model, (b) 0° model.*

For the stress distribution of the 0° specimen, shown in Figure 12(b), σ_x is the stress in the longitudinal direction of fiber tow; σ_y is the stress in the transverse direction to the fiber tow, and τ_{xy} is the in-plane shear stress. In this case, the crack is perpendicular to stress direction of σ_y (Figure 11). As mentioned, the strength of composite in tow orientation is much higher than that in other directions. Therefore, although there is a significant amount of σ_x comparing to other components, we believe, as was seen for the 90° specimen, that the initial failure is in the epoxy resin phase, either inside the tow or between tows, caused by σ_y or τ_{xy}. This argument can also be supported by the information presented in Table 5.

Table 5 lists the applied shear stress ($\bar{\tau}$) values at the onset of crack initiation located near the notch root for two hybrid systems with both 90 and 0° specimens. One can see from the table, within experimental uncertainty, that the shear stresses corresponding to the crack initiation are dependent on tow orientations but not carbon content. For 90° specimen, at the onset of crack initiation the average ($\bar{\tau}$) is about 35.3 MPa (obtained by averaging the stresses listed in Table 5), which induces a tensile stress of 47.0 MPa (35.3×1.33, using

Table 5. The shear stress corresponding to the onset of crack initiation near the notch root.

Hybrid Composite Systems	Shear Stress (MPa) 0° Specimen	Shear Stress (MPa) 90° Specimen
Low carbon	44.2 ± 0.78	33.1 ± 0.81
High carbon	46.4 ± 2.48	37.4 ± 1.41

Figure 12). For 0° specimen, at the onset of crack initiation the average applied shear stress, $\bar{\tau}$, is about 45.3 MPa (also obtained by averaging the stresses listed in Table 5), which induces to a tensile stress of 49.0 MPa (45.3×1.09). Within experimental uncertainty, these two tensile stresses (49.0 and 47.0 MPa, transverse to tow orientations) corresponding to the onset of crack initiation near the notch root in 90 and 0° specimens are almost identical. These values also fall into the ball park of tensile strength of epoxies at room temperature, which was reported at the range of 30–50 MPa, while the shear strength are 60–80 MPa [14]. This further suggests that both failure initiations in 90 and 0° specimens just occurred by the tensile failure of epoxy matrix. From the above inference based on the FEA and strength of materials evidence, one can assume that the crack initiation near the notch root of 0° specimen is a mixed mode but dominated by the opening mode. Furthermore, this is a validation of the previous speculation that the onset of crack initiation near the notch root in 90° specimen is dominated by the opening mode.

CONCLUSION

Using the v-notch shear test with the modified Wyoming test fixture, the in-plane shear properties of unidirectional hybrid composite were evaluated analytically and experimentally. The v-notch specimen of hybrid composite contains carbon–epoxy and glass–epoxy tows in 0 and 90° directions. From the study, we determined that although the local inhomogeneity inherent in the hybrid composites affects the composite mechanics in the v-notch specimen, the test (at least for the unidirectional hybrid composites used in this study) still exhibits a limited region possessing a reasonably pure and uniform stress–strain state between the notches to meet the requirement for determining the in-plane shear modulus and strength. Thus, the study indicates that the v-notch test can be used for the shear testing of the hybrid composites when it is correctly used. Based on experimental observations and the FEA, 90° specimens have better purity and uniformity than 0° specimens in shear stress distribution over test region.

Due to stress concentrations caused by the existence of geometry and material discontinuities at the free edges of the notches, it is highly possible that premature failure of the specimen can occur in the notch tip area. We believe that those premature failures, which are sensitive to the stress concentration in the notch area, observed in our 0 and 90° specimens are associated with a mixed-mode failure, but dominated by the opening mode. It is not rigorous for us to interpret the shear strength based on the information of the crack initiation occurred in the premature failures. Therefore, at this stage, we conclude that v-notch shear test is effective for the evaluation of the shear modulus, but not for the shear strength, of the unidirectional hybrid composites used in this study. Finally, the study also demonstrates that the shear modulus of unidirectional hybrid composites is dominated by the matrix content (no hybrid effect), as it does for nonhybrid composites.

REFERENCES

1. Iosipescu, N. (1967). New Accurate Procedure for Single Shear Testing of Metals, *Journal of Materials*, **2**(3): 537–566.
2. Adams, D.F. and Thomas, R.L. (1969). The Solid-Rod Torsion Test for the Determination of Unidirectional Composite Shear Modulus, *Textile Res. J.*, **39**(4): 339–345.
3. Swanson, S.R., Messick, M. and Toombes, G.R. (1985). Comparison of Torsion Tube and Iosipescu In-Plane Shear Test Results for a Carbon Fiber-Reinforced Epoxy Composite, *Composites*, **16**: 220–224.
4. Walrath, D.E. and Adams, D.F. (1982). The Iosipescu Shear Test as Applied to Composite Materials, *Experimental Mechanics*, **27**(2): 105–110.
5. Adams, D.F. and Walrath, D.E. (1987). Further Development of the Iosipescu Shear Test Method, *Experimental Mechanics*, **27**(2): 113–119.
6. Barnes, J.A., Kumosa, M. and Hull, D. (1987). Theoretical and Experimental Evaluation of the Iosipescu Shear Test, *Composites Science and Technology*, **28**: 251–268.
7. Morton, J., Ho, H., Tsai, M.Y. and Farley, G.L. (1992). An Evaluation of the Iosipescu Specimen for Composite Materials Shear Property Measurement, *Journal of Composite Materials*, **26**(5): 708–750.
8. Xing, Y.M., Poon, C.Y. and Ruiz, C. (1993). A Whole-Field Strain Analysis of the Iosipescu Specimen and Evaluation of Experimental Errors, *Composites Science and Technology*, **47**: 251–259.
9. Bansal, A. and Kumosa, M. (1995). Experimental and Analytical Studies of Failure Modes in Iosipescu Specimens under Biaxial Loadings, *Journal of Composite Materials*, **29**(3): 334–358.
10. Pierron, F. and Vautrin, A. (1997). Measurement of the In-Plane Shear Strength of Unidirectional Composites with the Iosipescu Test, *Composite Science and Technology*, **57**: 1653–1660.
11. Standard Test Method for Shear Properties of Composite Materials by the V-notched Beam Method, *ASTM Standard D5379-93*, American Society for Testing and Materials, Philadelphia. (May 1993).
12. Chiang, M.Y.M. and He, J. An Analytical Assessment of Using the Iosipescu Shear Test for Hybrid Composites, *Composites: Part B*, **33**(6): 461–470.
13. ABAQUS (2000). Finite Element Analysis Code and Theory (Standard and CAE), Version 6.1. Hibbitt, Karlsson & Sorensen, Inc., RI, USA.
14. Tsai, Stephen W. (1980). *Introduction of Composite Materials – Chapter 9*: *Micromechanics*, pp. 388–401, Technomic Publishing Co., Inc., Westport, CT, USA.
15. He, J., Chiang, M.Y.M. and Hunston, D.L. (2001). Assessment of Sandwich Beam in Three-Point Bending for Measuring Adhesive Shear Modulus, Transaction of the ASME, *Journal of Engineering Material and Technology*, **123**: 1–7.
16. Chiang, M.Y.M. and Chai, H. (1994). Plastic Deformation Analysis of Cracked Adhesive Bonds Loaded in Shear, *Int. J. Solids Structures*, **31**: 2477–2490.